

**Zeitschrift:** IABSE congress report = Rapport du congrès AIPC = IVBH  
Kongressbericht

**Band:** 2 (1936)

**Artikel:** Secondary stresses in triangulated steel structures

**Autor:** Ridet, J.

**DOI:** <https://doi.org/10.5169/seals-3213>

### **Nutzungsbedingungen**

Die ETH-Bibliothek ist die Anbieterin der digitalisierten Zeitschriften auf E-Periodica. Sie besitzt keine Urheberrechte an den Zeitschriften und ist nicht verantwortlich für deren Inhalte. Die Rechte liegen in der Regel bei den Herausgebern beziehungsweise den externen Rechteinhabern. Das Veröffentlichen von Bildern in Print- und Online-Publikationen sowie auf Social Media-Kanälen oder Webseiten ist nur mit vorheriger Genehmigung der Rechteinhaber erlaubt. [Mehr erfahren](#)

### **Conditions d'utilisation**

L'ETH Library est le fournisseur des revues numérisées. Elle ne détient aucun droit d'auteur sur les revues et n'est pas responsable de leur contenu. En règle générale, les droits sont détenus par les éditeurs ou les détenteurs de droits externes. La reproduction d'images dans des publications imprimées ou en ligne ainsi que sur des canaux de médias sociaux ou des sites web n'est autorisée qu'avec l'accord préalable des détenteurs des droits. [En savoir plus](#)

### **Terms of use**

The ETH Library is the provider of the digitised journals. It does not own any copyrights to the journals and is not responsible for their content. The rights usually lie with the publishers or the external rights holders. Publishing images in print and online publications, as well as on social media channels or websites, is only permitted with the prior consent of the rights holders. [Find out more](#)

**Download PDF:** 07.08.2025

**ETH-Bibliothek Zürich, E-Periodica, <https://www.e-periodica.ch>**

## V 12

### Secondary Stresses in Triangulated Steel Structures.

### Nebenspannungen in Dreiecksfachwerken.

### Efforts secondaires dans les ouvrages triangulés.

J. Ridet,

Ingénieur en Chef Adjoint, Chemins de fer de l'Est, Paris.

#### I. General Conditions.

In an earlier note the Author has described his researches relating to secondary stresses caused by the rigidity of the connections in trussed structures of reinforced concrete. The object of these researches was to check experimentally certain formulae giving the values of the secondary stresses in question. The formulae arrived at two different methods show but little difference in the results.

It appeared worth while, as suggested in the earlier note, to proceed to similar experiments on a steel bridge. Now it might appear evident, from the beginning, that in a trussed girder of reinforced concrete the secondary stresses arising through the members being fixed in one another would be greater than in a steel girder, because all reinforced concrete construction forms a true monolith in which such fixing action is almost perfectly realised. It will be seen later, however, that this is by no means the case.

There is no occasion to repeat here the principles that serve as the theoretical basis for determining secondary stresses, and the Author will confine himself to describing the experiments which have been carried out and to stating their results and the conclusions which may be drawn from them.

#### II. Choice and Description of the Structure.

In order to be able to compare the experiments as between the two bridges, one in reinforced concrete and one in steel, it was necessary that each structure should have a span of the same order, that the two girders should be of the same type, and that the live loads imposed on them should be similar.

With this object — on the advice of M. *Cambournac*, chief engineer for Works and Maintenance of the Nord Railway — the choice fell on a bridge in the disused line from Douai to Leforest crossing the Haute-Deule Canal at Douai. This is a skew bridge of 40 metres square opening, carrying two tracks over the canal on two separate bridge floors which are identical but independent of one another. Plate 1 shows the general arrangement of one of these floors.


The girders are of 43.540 metres span and are 5 metres high. The lower boom is horizontal and the upper boom is also horizontal except in the end panels which are inclined so as to connect with the lower boom over the supports.

The girders are connected with one another at the bottom by floor beams carrying two lines of rail bearers which in turn carry the track on sleepers. The booms of the two girders are connected at the top by horizontal wind-bracing.

### III. Apparatus Used for the Measurements: Position and Fixing.

The same apparatus were used as had been applied to the reinforced concrete structure, namely extensometers by *Manet-Rabut*, *Huggenberger* and *Mabboux*, which need not be described again here. These instruments were placed as in Fig. 1 — on the diagonal AC close to the joint C; on the vertical BC close to the joints and at the middle M; on the diagonal BD close to the joint B and at the middle N. The *Manet-Rabut* and *Huggenberger* instruments are attached in a very simple way by means of the fittings provided on them; but special clamps had to be made for the attachment of the *Mabboux* apparatus and these are represented in Plate II.

Plates III and XI show the positions of the various types of instrument as affixed to the diagonals and the vertical, the positions having been so chosen as to ensure that, as far as possible, the maximum forces in each section would be measured. With the *Mabboux* instrument it was not possible to make the measurements as complete as with the other instruments as no scaffolding could be erected on the inside of the bridge which had to be left free for the passage of locomotives.

In the verticals the cross-section is of a special type thus:  the middle part, fixed to the web of the girder, receiving the stress directly and transmitting it to the remainder. It was therefore of interest, to measure the secondary stresses in each of the branches, and with this object, whenever possible, apparatus were attached to all the three branches. The importance of these measurements will appear later.

### IV. Execution of the Experiments.

The experiments were carried out by loading the bridge with two locomotives of the "Consolidation" type, each having a tender of 34 m<sup>3</sup> capacity, as used on the Réseau du Nord — the same type as was used in the experiment on the reinforced concrete bridge at St.-Ouen. The total weight of each locomotive with its tender was 155 tons.

All the measurements were taken with the locomotive in the same position on the bridge giving very nearly the maximum stresses in the members under examination. The rear axle of the tender was placed to the right of the vertical BC (Fig. 1) so that the load covered the greater part of the bridge.

A scaffold with three storeys was hung from the girders in such a way as to allow the instruments to be easily read, and these were placed successively on each of the parts which it was proposed to investigate.

### V. Results and Discussion of the Experiments.

The tables in Plates III to XI show the stresses measured by the various instruments in the course of the experiments, in kg per sq. mm.

The *Manet-Rabut* instrument measured variations in length on a gauge length of 0.110 metre, the *Huggenberger* instrument on a length of 0.020 metre and the *Mabboux* instrument on a length of 0.050 metre. To render the results comparable all the measurements were referred to a length of 0.020 metre so that every variation of  $1\mu$  corresponds to a stress of 1 kg per sq. mm.

As in the experiments on the reinforced concrete bridge at St.-Ouen, the instruments nearly always returned exactly to the starting position after the load had been removed.

The table given below shows the results, in kg per sq. mm, for the calculated secondary stresses at the ends A and B of each of the three members examined. In this table  $n_a$  and  $n_b$  are the principal stresses in the bars while  $n$  and  $n_B$  are the respective secondary stresses at the ends A and B of the bars. The table also shows the ratio between the secondary stress and the calculated principal stress, as found according to the two methods of M. Fontviolant and M. Pigeaud respectively.

Designation of members	Principal stresses $n_a$ or $n_b$ (calculated)	Stresses as calculated by the Fontviolant method		Stresses as calculated by the Pigeaud method	
		Secondary stresses $n_A$ or $n_B$	$\frac{n_A}{n_a} \times 100$ or $\frac{n_B}{n_b} \times 100$	Secondary stresses $n_A$ or $n_B$	$\frac{n_A}{n_a} \times 100$ or $\frac{n_B}{n_b} \times 100$
Diagonal AC point A	— 2.83	$\pm 1.04$	37	$\pm 0.79$	28
in tension point B	— 2.83	$\pm 0.89$	31	$\pm 0.79$	27
Vertical BC point A	1.81	$\pm 1.15$	64	$\pm 1.08$	60
in compression point B	1.81	$\pm 1.26$	70	$\pm 1.13$	62
Diagonal BD point A	— 3.27	$\pm 1.28$	39	$\pm 1.28$	39
in tension point B	— 3.27	$\pm 1.30$	40	$\pm 1.05$	32

The information given in this table has reference to sections of the bars at the theoretical truss-point, as if there were no gussets, and the figures obtained make it possible to plot diagrams of the theoretical stresses as in Plates Nos XII and XIII.

The indications given in tables on Plates III and XI do not correspond to the maximum values of the secondary stresses because the apparatus could not always be so applied as to measure the most heavily stressed fibres of the sections; that is, the furthest fibres from the neutral axis. For the purpose of determining the probable real stress in these fibres it has been assumed that



the stress varies between the extreme fibres of each section according to a linear law, and the calculation has been made as follows:

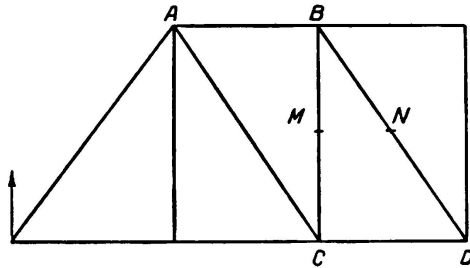


Fig. 1.

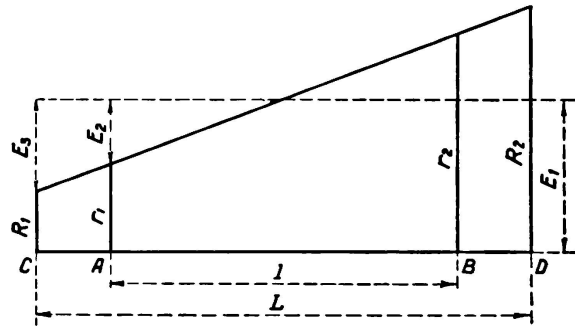


Fig. 2.

Knowing the measured values of stresses  $r_1$  and  $r_2$  at the points A and B separated by a distance  $l$  (Fig. 2) the mean stress in the member has been calculated; this corresponds to the stress due to the principal force and has the value

$$E_1 = \frac{r_1 + r_2}{2}$$

Hence the secondary stress  $E_2$  which results from these measurements is

$$E_2 = \pm (E_1 - r_1)$$

and the maximum calculated secondary stress  $E_3$  in the extreme fibres C and D separated by a distance  $L$  is  $E_3 = \pm E_2 \times \frac{L}{l}$ . Hence the total stresses in the extreme fibres are

$$R_1 = E_1 - E_3 \text{ and } R_2 = E_1 + E_3$$

The tables which follow give the following measurements as obtained by the different instruments (with the exception of those fixed to the middle of the length of the bars where the secondary stress is very small): the principal stress  $n_a$  or  $n_b$ ; the average stress resulting from the measurements  $E_1$ ; the secondary stresses  $E_2$  and  $E_3$ ; the value  $\frac{E_3}{E_1} \times 100$ , and finally the total stresses  $R_1$  and  $R_2$ . (For the position of the instruments see Plates III and XI).

Section on right of instruments	Calculated principal stress $n_a$ or $n_b$	Measured principal stress $E_1$	Measured secondary stress $E_2$	Maximum secondary stress $E_3$	$\frac{E_3}{E_1} \times 100$	Total stresses	
						$R_1$	$R_2$

#### MANET-RABUT EXTENSOMETERS

##### Upperporotin

I - II	+ 1.81	+ 1.56	$\pm 1.06$	$\pm 1.88$	120	- 0.32	3.44
III - IV	+ 1.81	+ 1.75	$\pm 2.29$	$\pm 2.60$	148	- 0.85	4.35
V - VI	+ 1.81	+ 1.34	$\pm 1.25$	$\pm 2.22$	166	- 0.88	3.56
VII - VIII	- 3.27	- 2.68	$\pm 0.82$	+ 0.82	31	- 3.50	- 2.04
IX - X	- 3.27	- 2.46	$\pm 1.04$	$\pm 1.04$	42	- 3.50	- 1.42

Section on right of instruments	Calculated principal stress $n_a$ or $n_b$	Measured principal stress $E_1$	Measured secondary stress $E_2$	Maximum secondary stress $E_3$	$\frac{E_3}{E_1} \times 100$	Total stresses	
						$R_1$	$R_2$
Lower portion							
I—II	+ 1.81	+ 1.24	$\pm$ 0.88	$\pm$ 1.56	126	— 0.32	2.80
III—IV	+ 1.81	+ 1.80	$\pm$ 1.62	$\pm$ 1.84	102	— 0.04	3.64
V—VI	+ 1.81	+ 1.27	$\pm$ 0.86	$\pm$ 1.53	120	— 0.26	2.80
VII—VIII	— 2.83	— 1.66	$\pm$ 0.16	$\pm$ 0.16	10	— 1.82	— 1.50
IX—X	— 2.83	— 1.93	+ 0.70	+ 0.70	36	— 2.63	— 1.23

## HUGGENBERGER EXTENSOMETERS

Upper portion							
1—2	+1.81	+1.12	$\pm 0.62$	$\pm 1.10$	98	+0.02	+2.22
3—4	+1.81	+1.38	$\pm 0.63$	$\pm 1.12$	81	-0.26	+2.50
5—6	+1.81	+1.38	$\pm 1.38$	$\pm 1.57$	114	-0.19	+2.95
7—8	+1.81	+1.12	$\pm 1.12$	$\pm 1.27$	114	-0.15	+2.39
9—10	+1.81	+0.88	$\pm 0.88$	$\pm 1.56$	177	-0.68	+2.44
11—12	+1.81	+1.00	$\pm 0.75$	$\pm 1.33$	133	-0.33	+2.33
13—14	-3.27	-2.62	$\pm 0.87$	$\pm 0.87$	33	-3.49	-1.75
15—16	-3.27	-2.12	$\pm 0.87$	$\pm 0.87$	41	-2.99	-1.25
17—18	-3.27	-2.12	$\pm 0.87$	$\pm 0.87$	41	-2.99	-1.25
19—20	-3.27	-2.38	$\pm 0.63$	$\pm 0.63$	26	-3.01	-1.75

Lower portion							
1—2	+1.81	+1.12	$\pm 0.62$	$\pm 1.10$	98	+0.02	+2.22
3—4	+1.81	+0.88	$\pm 0.38$	$\pm 0.67$	76	+0.15	+1.26
5—6	+1.81	+1.25	$\pm 1.00$	$\pm 1.14$	91	+0.11	+2.39
7—8	+1.81	+1.25	$\pm 1.25$	$\pm 1.42$	114	-0.17	+2.67
9—10	+1.81	+1.00	$\pm 0.50$	$\pm 0.89$	89	+0.11	+1.89
11—12	+1.81	+1.00	$\pm 0.50$	$\pm 0.89$	89	+0.11	+1.89
13—14	-2.83	-1.75	$\pm 0.50$	$\pm 0.50$	29	-1.75	-1.25
15—16	-2.83	-1.75	$\pm 0.50$	$\pm 0.50$	29	-1.75	-1.25
17—18	-2.83	-1.62	$\pm 0.63$	$\pm 0.63$	39	-2.25	-0.99
19—20	-2.83	-1.62	$\pm 0.63$	$\pm 0.63$	39	-2.25	-0.99

## MABBOUX EXTENSOMETERS

Upper portion							
A—B	+1.81	+1.85	$\pm 0.55$	$\pm 0.98$	53	0.87	2.83
C—D	+1.81	+1.70	$\pm 0.80$	$\pm 1.42$	83	0.28	3.12
E—F	+1.81	+1.95	$\pm 1.45$	$\pm 1.64$	84	0.31	3.59
G—H	+1.81	+1.50	$\pm 1.30$	$\pm 1.47$	98	0.03	2.97
I—J	-3.27	-2.80	$\pm 0.70$	$\pm 0.90$	32	-3.70	-1.90
K—L	-3.27	-3.05	$\pm 0.55$	$\pm 0.71$	23	-3.76	-2.34
Lower portion							
A—B	+1.81	+1.40	$\pm 0.50$	$\pm 0.89$	63	0.51	2.29
C—D	+1.81	+1.40	$\pm 0.60$	$\pm 1.06$	76	0.34	2.46
E—F	+1.81	+1.60	$\pm 1.00$	$\pm 1.14$	71	0.46	2.74
G—H	+1.81	+1.50	$\pm 1.20$	$\pm 1.36$	91	0.14	2.86
I—J	-2.83	-1.70	$\pm 0.20$	$\pm 0.34$	20	-2.04	-1.36
K—L	-2.86	-2.20	$\pm 0.50$	$\pm 0.83$	38	-3.03	-1.37

### *Accuracy of the Measurements.*

The variations in length measured by the instruments are extremely small, rarely reaching as much as  $4 \mu$ . Hence even a small error in the reading has a considerable effect on the results. Consider, for instance, the instruments 9 and 10 affixed to the upper portion of the vertical. The readings taken on these instruments were 0 in the case of N° 9 and  $-1.75$  in the case of N° 10. Assuming an error of  $\frac{1}{4} \mu$  in the reading of instrument N° 9 so that instead of reading 0 the reading has been  $-0.25$ , then the result would be as follows:

$$E_1 = -1 \quad E_2 = \pm 0.75 \quad E_3 = \pm 1.33$$

and

$$\frac{E_3}{E_1} \times 100 = 133 \text{ instead of } 177$$

The fact that no anomalies like this have been recorded is probably due to the readings taken on the *Mabboux* instruments being more accurate.

Examination of the tables leads to the following facts being established:

- 1) *Comparison between the principal stress as calculated and the principal stress as measured.*

The principal stress  $E_1$  as measured in a member is less than the principal stress  $n_a$  or  $n_b$  as calculated by about 28 %, this percentage being obtained by taking the mean of the measurements.

Such a case is general. The difference between the calculated stresses and the measured stresses is a consequence largely of the rigidity of the floor elements (rail bearers, rails, etc.) of which no account was taken in the calculations.

- 2) *Secondary stresses.*

#### *A. In the diagonals.*

In the diagonals, whatever the instrument used, the secondary stress as measured remains within the normal limit and does not exceed 42 % of the principal stress as measured. Plate XII shows that the secondary stresses as measured are always less than the secondary stresses as calculated, the mean difference being about 38 %.

#### *B. In the verticals.*

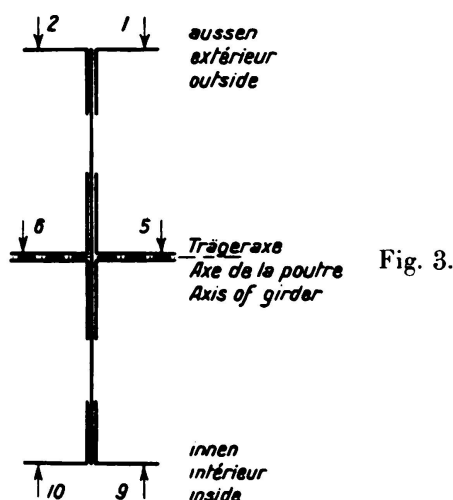
The same is not true of the verticals. The results obtained from the several instruments do not agree, for with the *Mabboux* instruments the secondary stresses as measured = 98 % of the principal stress as measured, while with the *Manet-Rabut* instrument the proportion is as high as 166 %, and in the *Huggenberger* as high as 177 %. Apart from this, appreciably different results were obtained when the same series of instruments was placed on the same section in turn.

The secondary stresses do not cause an increase of more than 2.6 kg per sq. mm to the principal stress and the total maximum stress is 4.35 kg per sq. mm, which is therefore far below the plastic limit.

An attempt will be made to explain these results by studying the section in which the instruments 1—2, 5—6 and 9—10 are attached in the upper part of the vertical.

a) *Effect of the method of attachment on the distribution of stresses in a given section.*

As already stated, the vertical member has the section represented here in Plate III and is connected to the web of the girder by means of central angle bars. The six instruments were attached as follows:



- 1 and 2 of the outside face of the vertical.
- 5 and 6 on the central angle bars.
- 9 and 10 on the inside face.

On comparing the values of the  $E_1$  in these three groups they were found to be respectively 1.12, 1.38 and 0.88.

It was at once concluded that owing to the art of construction the stress in the vertical is not uniformly distributed over the whole section, but the portion *directly attached to the web* takes the greatest share.

*Comparison with a joint in reinforced concrete structure.*

In a reinforced concrete panel-point the distribution of stresses should take place much more favourably, because both compressive and tensile stresses are transmitted within the connection itself through the concrete and the reinforcements. If the connection has been properly designed the elementary stresses meet one another at the actual points of intersection, where they stand in equilibrium, having therefore no resultant-force to be transmitted. This is why, in reinforced concrete — apart from the fact that no rivets are required — there is no necessity for a gusset. Moreover in reinforced concrete there is no need to fear eccentricity of the connection.

b) *Stiffening effect of the floor construction in through girders.*

There is a further consideration which helps to explain why the values of  $E_1$  differ appreciably as between the inside and the outside of the girder:

taking a cross section of the bridge through one of the floor beams, it will be seen that the verticals, the floor beams and the upper wind bracing constitute a frame which deforms under the passage of the load, as indicated in Fig. 4.

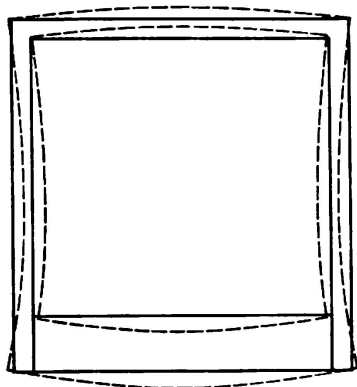


Fig. 4.

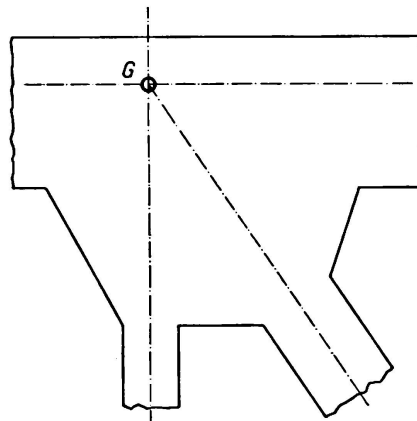


Fig. 5.

The verticals are subjected to bending moments in a plane normal to the girder, and these cause tension on the inside and compression on the outside face. As the vertical is normally in compression, it is easy to understand that the mean stress  $E_1 = 1.12$  in the case of instruments 1—2 placed on the outside would be larger than the mean stress  $E_1 = 0.88$  measured by the instruments 9—10.

Moreover, the secondary stresses  $E_3$  corresponding to the three groups have absolute values of 1.10, 1.57 and 1.56: that is to say they represent respectively 98 %, 114 % and 177 % of  $E_1$ . It will be observed that the absolute values do not differ very much in the case of the last two, but they have reference to widely varying values of  $E_1$ , which goes to explain the very high percentage of secondary stresses for the inside faces.

### c) Effect of Gussets.

The secondary stresses are calculated on the assumption that the bars are rigidly fixed at the point of intersection  $G$  which is the centre of gravity of the boom, the length being calculated from joint to joint. It is not possible in these calculations to take account of the large gussets by which the boom members, the verticals, and the diagonals are connected with one another (Fig. 5).

It is clear, however, that the gussets exert an influence: —

1) Because the angular displacements cannot in fact take place in accordance with the assumption on which the calculation is based.

2) Because the *slenderness* of the bars (the proportion of their length to their width) varies considerably according as the length is measured from intersection to intersection or is taken as the distance *between gussets*. For instance, in the case of the vertical under consideration (middle portion) the ratio of slenderness assumed in the calculations is 23.5, but if it were measured by reference to the length between gussets it would be only 14.25. For the corresponding vertical on the reinforced concrete bridge at St. Ouen, as previously investigated, the ratio of slenderness was 14.0 if calculated on the length between intersections

and 11.1 if referred to the measurement between the edges of the booms (there being no gusset).

In the case of the diagonals, the ratio of slenderness used in the calculations was 17.7 and the true ratio of slenderness was 11.9.

3) Finally, it is a question whether the gusset, with its rivets and its inertia varying from one point to another, does in fact transmit the compressive and tensile stresses in accordance with the intersecting straight lines which we have assumed.

It is true that, in properly designed connections, the centre lines of the rivets run along the neutral axes of the vertical or diagonal members concerned, but the moment of inertia of these members projecting over the gussets is variable, also the position of the centre of gravity of the sections, that the distribution of elementary stresses in a section of the gusset may be disturbed.

These considerations suggest the idea that when examining gussets by photoelasticity the models might with advantage not be made plane, as is ordinarily done for the purpose of studying a complete structure, but should be thickened at the places where the transverse inertia is increased.

It is to be desired that other experiments may be carried out in order to confirm these conclusions.

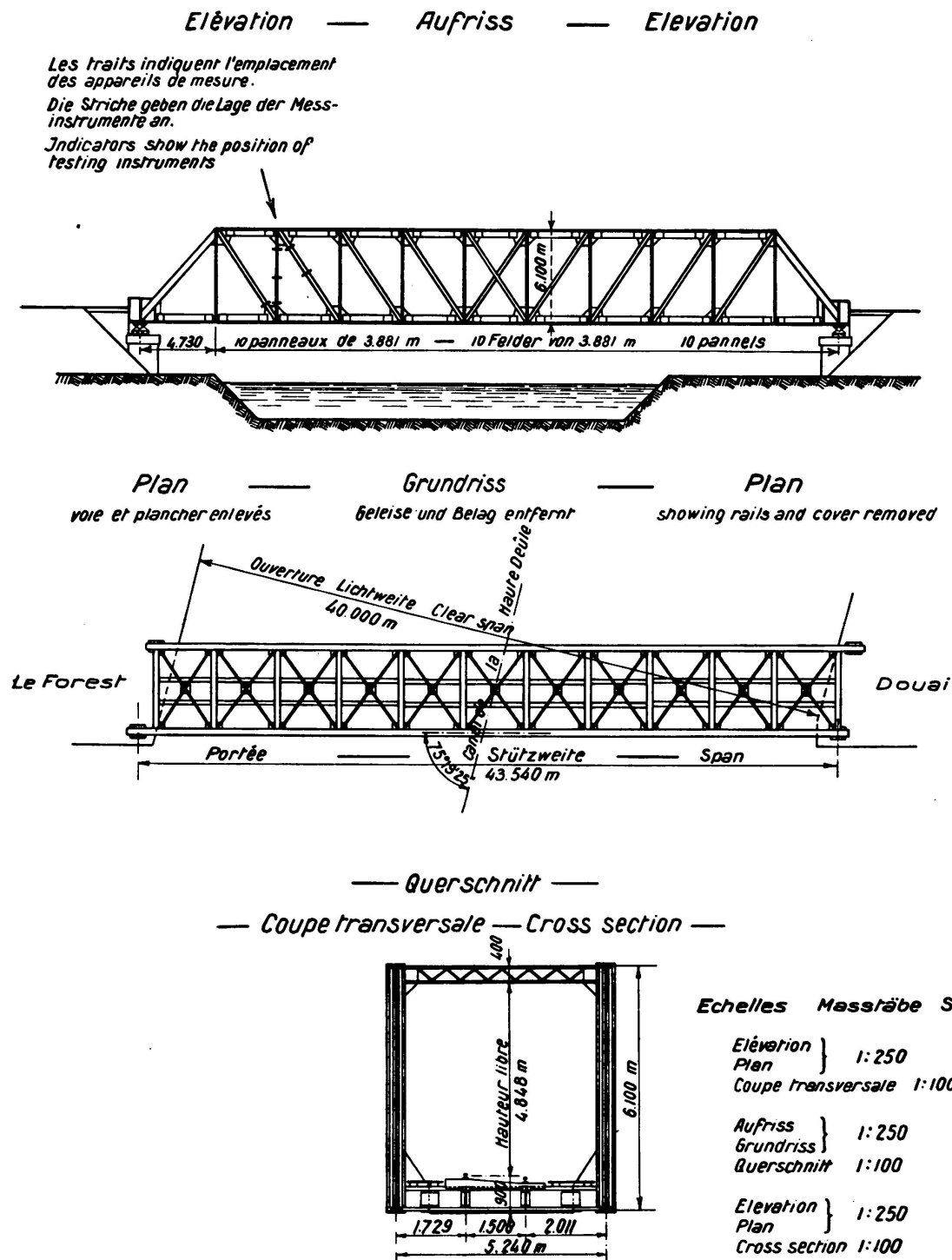


Table I.

Bridge over the Haute-Deule-Canal at Douai. (Douai to Laforest.)

General arrangement.

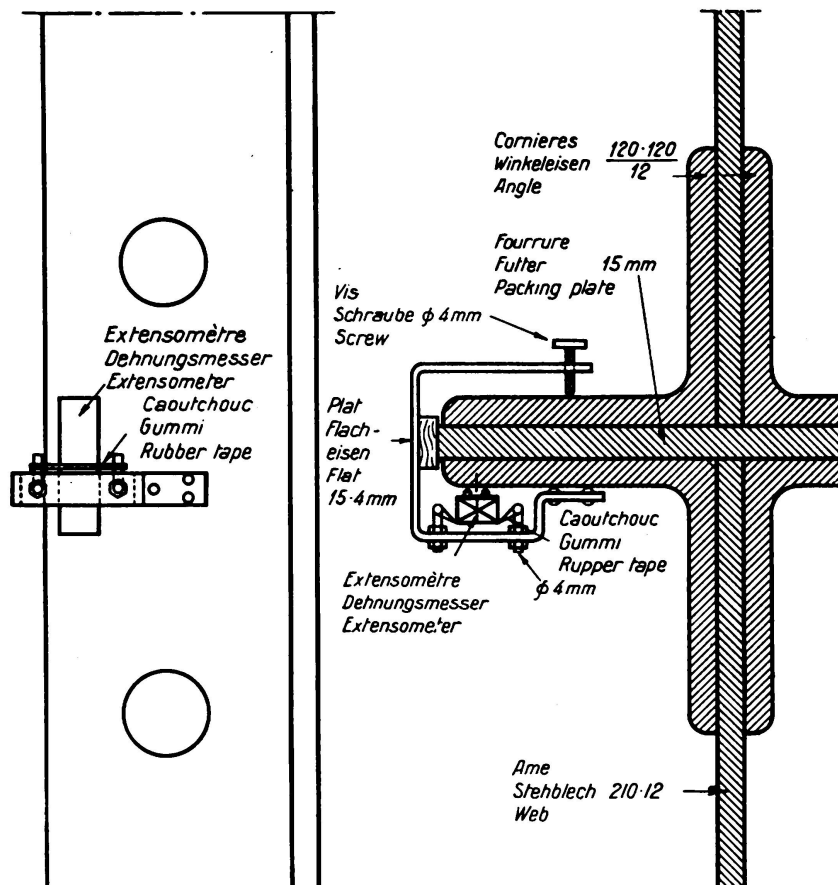


Table II.

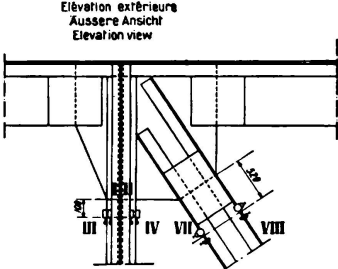
Tests carried out at the Douai bridge. Mode of fixing Mabboux extensometers to verticals.  
(Central angle irons).



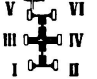
Upper parts of  
main girder.Extensometers Manet-Rabut  
(Base 0,02 m)

Table III.

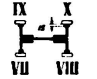
Position of Instruments				stresses in kg/mm <sup>2</sup>	
				— tension	+ compression
				measured	calculated
Vertical	outer angle iron $\overline{A}$	I		+ 0,50	+ 1,43
		II		+ 2,63	+ 2,19
	central angle iron	III		— 0,54	+ 1,22
		IV		+ 4,04	+ 2,40
	inner angle iron $\overline{R}$	V		+ 0,09	+ 1,43
		VI		+ 2,59	+ 2,19
Diagonal	outer angle iron $\overline{A}$	VII		— 3,50	— 3,98
		VIII		— 1,86	— 2,56
	inner angle iron $\overline{R}$	IX		— 3,50	— 3,98
		X		— 1,41	— 2,56



Elévation extérieure  
Aussere Ansicht  
Elevation view



Section du montant  
Querschnitt des Pfostens  
Cross section of vertical post

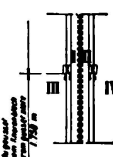


Section de la diagonale  
Querschnitt der diagonale  
Cross section of diagonal member


Middle parts of  
main girder.Extensometers Manet-Rabut  
(Base 0,02 m)

Table IV.

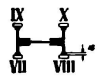
Position of Instruments				stresses in kg/mm <sup>2</sup>	
				— tension	+ compression
				measured	calculated
Vertical	outer angle iron $\overline{A}$	I		+ 1,54	+ 1,81
		II		+ 1,27	+ 1,81
	central angle iron	III		+ 1,59	+ 1,81
		IV		+ 1,45	+ 1,81
	inner angle iron $\overline{R}$	V		+ 1,77	+ 1,81
		VI		+ 1,36	+ 1,81
Diagonal	outer angle iron $\overline{A}$	VII		— 2,36	— 3,33
		VIII		— 2,63	— 3,21
	inner angle iron $\overline{R}$	IX		— 2,41	— 3,33
		X		— 2,54	— 3,21



Elévation extérieure  
Aussere Ansicht  
Elevation view



Section du montant  
Querschnitt des Pfostens  
Cross section of vertical post

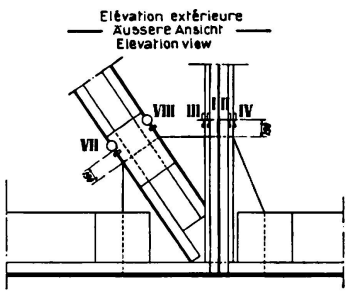


Section de la diagonale  
Querschnitt der diagonale  
Cross section of diagonal member


Lower parts of  
main girder.Extensometers Manet-Rabut  
(Base 0,02 m)

Table V.

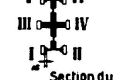
Position of Instruments				stresses in kg/mm <sup>2</sup>	
				— tension	+ compression
				measured	calculated
Vertical	outer angle iron $\overline{A}$	I		+ 2,13	+ 2,14
		II		+ 0,36	+ 1,48
	central angle iron	III		+ 3,41	+ 2,33
		IV		+ 0,18	+ 1,29
	inner angle iron $\overline{R}$	V		+ 2,13	+ 2,14
		VI		+ 0,41	+ 1,48
Diagonal	outer angle iron $\overline{A}$	VII		— 1,50	— 2,37
		VIII		— 1,82	— 3,29
	inner angle iron $\overline{R}$	IX		— 1,23	— 2,37
		X		— 2,63	— 3,29



Elévation extérieure  
Aussere Ansicht  
Elevation view



Section de la diagonale  
Querschnitt der diagonale  
Cross section of diagonal member



Section du montant  
Querschnitt des Pfostens  
Cross section of vertical post

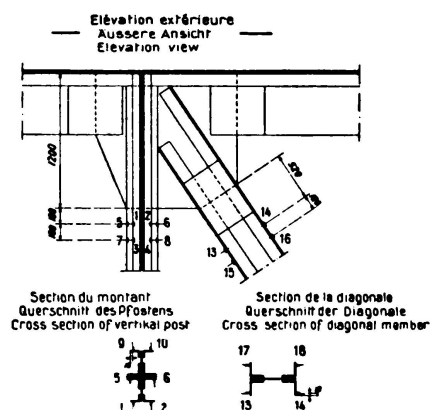
Upper parts of  
main girder.

## Extensometers Huggenberger

Table VI.

(Base 0,02 m)

Position of instruments			stresses in kg/mm <sup>2</sup>	
			— tension	+ compression
			measured	calculated
Vertical	outer angle iron $\overline{A}$	1	+ 0,50	+ 1,43
		2	+ 1,75	+ 2,19
		3	+ 0,75	+ 1,45
		4	+ 2,00	+ 2,17
	central angle iron	5	0	+ 1,22
		6	+ 2,75	+ 2,40
		7	0	+ 1,25
		8	+ 2,25	+ 2,37
	inner angle iron $\overline{R}$	9	0	+ 1,43
		10	+ 1,75	+ 2,19
		11	+ 0,25	+ 1,45
		12	+ 1,75	+ 2,17
Diagonal	outer angle iron $\overline{A}$	13	— 3,50	— 3,98
		14	— 1,75	— 2,56
		15	— 3,00	— 3,94
		16	— 1,25	— 2,60
	inner angle iron $\overline{R}$	17	— 3,00	— 3,98
		18	— 1,25	— 2,56
		19	— 3,00	— 3,94
		20	— 1,75	— 2,60

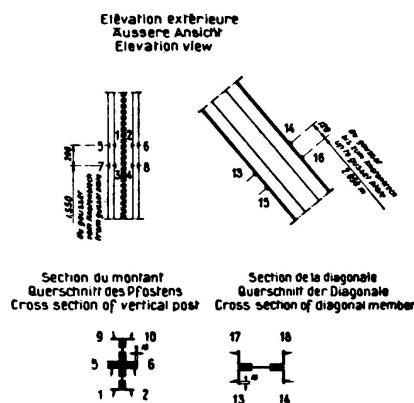
Middle parts of  
main girder.

## Extensometers Huggenberger

Table VII.

(Base 0,02 m)

Position of instruments			stresses in kg/mm <sup>2</sup>	
			— tension	+ compression
			measured	calculated
Vertical	outer angle iron $\overline{A}$	1	+ 1,25	+ 1,81
		2	+ 1,00	+ 1,81
		3	+ 1,50	+ 1,85
		4	+ 1,50	+ 1,77
	central angle iron	5	+ 1,25	+ 1,81
		6	+ 0,75	+ 1,81
		7	+ 1,25	+ 1,88
		8	+ 1,00	+ 1,74
	inner angle iron $\overline{R}$	9	+ 1,00	+ 1,81
		10	+ 0,75	+ 1,81
		11	+ 1,25	+ 1,85
		12	+ 1,00	+ 1,77
Diagonal	outer angle iron $\overline{A}$	13	— 2,00	— 3,33
		14	— 2,25	— 3,21
		15	— 2,25	— 3,29
		16	— 2,25	— 3,25
	inner angle iron $\overline{R}$	17	— 2,25	— 3,33
		18	— 2,50	— 3,21
		19	— 2,25	— 3,29
		20	— 2,25	— 3,25



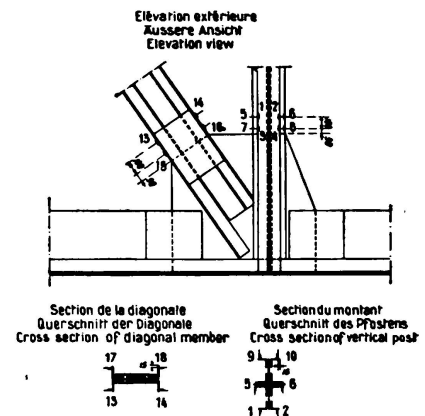
Lower parts of  
main girder.

## Extensometers Huggenberger

Table VIII.

(Base 0,02 m)

Position of instruments			stresses in kg/mm <sup>2</sup>	
			— tension	+ compression
			measured	calculated
Vertical	outer angle iron <i>A</i>	1	+ 1,75	+ 2,14
		2	+ 0,50	+ 1,48
		3	+ 1,25	+ 2,16
		4	+ 0,50	+ 1,46
	central angle iron	5	+ 2,25	+ 2,33
		6	+ 0,25	+ 1,29
		7	+ 2,50	+ 2,36
		8	0	+ 1,26
	inner angle iron <i>R</i>	9	+ 1,50	+ 2,14
		10	+ 0,50	+ 1,48
		11	+ 1,50	+ 2,16
		12	+ 0,50	+ 1,46
Diagonal	outer angle iron <i>A</i>	13	— 1,25	— 2,37
		14	— 2,25	— 3,29
		15	— 1,25	— 2,34
		16	— 2,25	— 3,32
	inner angle iron <i>R</i>	17	— 1,00	— 2,37
		18	— 2,25	— 3,29
		19	— 1,00	— 2,34
		20	— 2,25	— 3,32

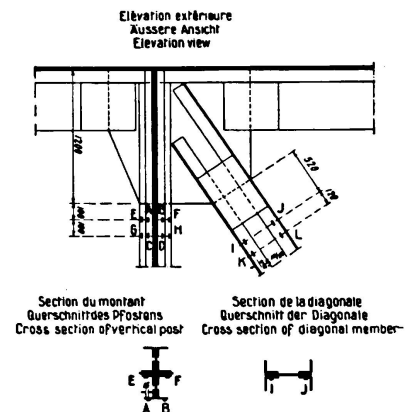
Upper parts of  
main girder.

## Extensometers Mabboux

Table IX.

(Base 0,02 m)

Position of instruments			stresses in kg/mm <sup>2</sup>	
			— tension	+ compression
			measured	calculated
Vertical	outer angle iron <i>A</i>	A	+ 1,30	+ 1,43
		B	+ 2,40	+ 2,19
		C	+ 0,90	+ 1,45
		D	+ 2,50	+ 2,17
	central angle iron	E	+ 0,50	+ 1,22
		F	+ 3,40	+ 2,40
		G	+ 0,20	+ 1,25
		H	+ 2,80	+ 2,37
Diagonal	inner legs of angle iron <i>A</i>	I	— 3,50	— 3,82
		J	— 2,10	— 2,72
		K	— 3,60	— 3,79
		L	— 2,50	— 2,75



Middle parts of  
main girder,


## Extensometers Mabboux

Table X

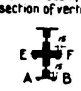
(Base 0,02 m)

Position of instruments			stresses in kg/mm <sup>2</sup>	
			— tension	+ compression
			measured	calculated
Vertical	outer angle iron <b>A</b>	A	+ 1,60	+ 1,81
		B	+ 1,10	+ 1,81
		C	+ 1,50	+ 1,85
		D	+ 1,60	+ 1,77
	central angle iron	E	+ 1,70	+ 1,81
		F	+ 1,25	+ 1,81
		G	+ 1,80	+ 1,88
		H	+ 1,50	+ 1,74

Elevation du montant  
Aufriss des Pfostens  
Elevation of the post



Section du montant  
Querschnitt des Pfostens  
Cross section of vertical post



Lower parts of  
main girder.

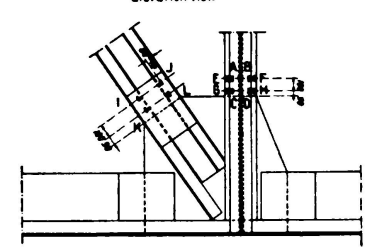
## Extensometers Mabboux

Table XI.

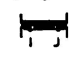
(Base 0,02 m)

Position of instruments			stresses in kg/mm <sup>2</sup>	
			— tension	+ compression
			measured	calculated
Vertical	outer angle iron <b>A</b>	A	+ 1,90	+ 2,14
		B	+ 0,90	+ 1,48
		C	+ 2,00	+ 2,16
		D	+ 0,80	+ 1,46
	central angle iron	E	+ 2,60	+ 2,33
		F	+ 0,60	+ 1,29
		G	+ 2,70	+ 2,36
		H	+ 0,30	+ 1,26
Diagonal	inner legs of angle iron <b>A</b>	I	— 1,50	— 2,55
		J	— 1,90	— 3,11
		K	— 1,70	— 2,54
		L	— 2,70	— 3,12


Elevation extérieure  
Außere Ansicht  
Elevation view



Section de la diagonale  
Querschnitt der Diagonale  
Cross section of diagonal member



Section du montant  
Querschnitt des Pfostens  
Cross section of vertical post



Effort principal calculé dû à la surcharge seule: Diagonale A-C: - 2.83 kg/mm<sup>2</sup>  
 Diagonale B-D: - 3.27 kg/mm<sup>2</sup>  
 Berechnete Hauptspannungen infolge allein der Verkehrslast: Diagonale A-C: 2.83 kg/mm<sup>2</sup>  
 Diagonale B-D: 3.27 kg/mm<sup>2</sup>  
 Calculated stresses due to external loadings only: Diagonal member A-C: - 2.83 kg/mm<sup>2</sup>  
 Diagonal member B-D: - 3.27 kg/mm<sup>2</sup>

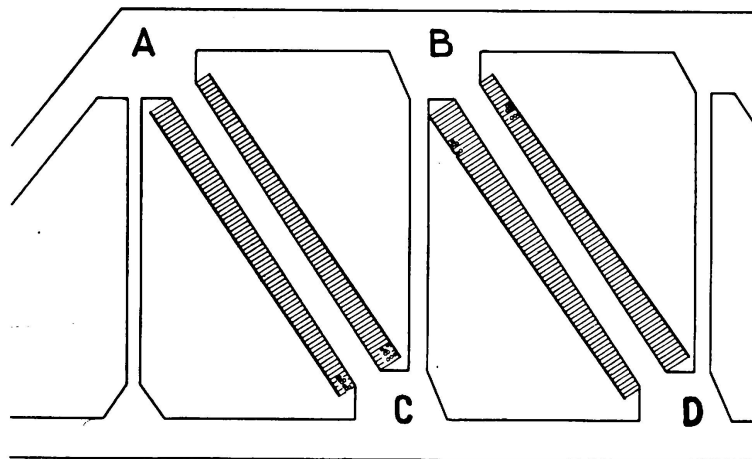


Table XII.

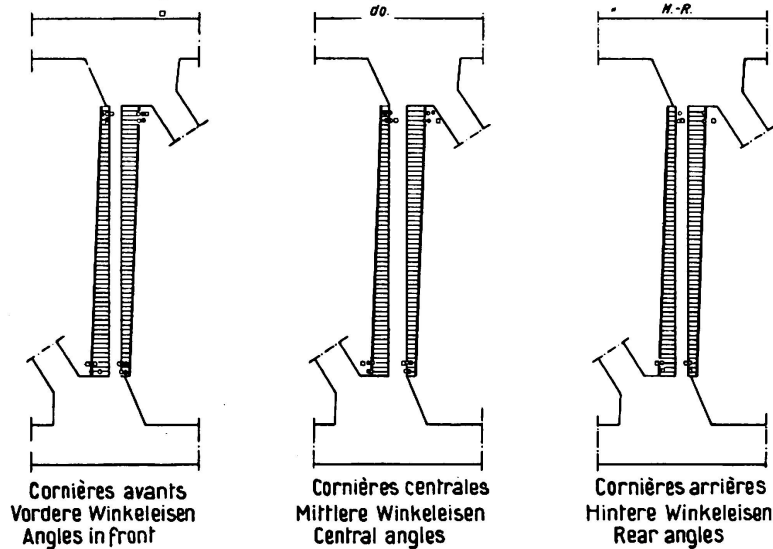
**Legende:**

- Effort total calculé (principal et second)  
 et dû à la surcharge seule 2<sup>e</sup> méthode  
 • Efforts mesurés (principal et second): app. Mabboux  
 do. : app. Huggenberger  
 do. : app. Manet-Rabut

**Illustration:**

- Calculated total stresses (principal and second)  
 due to traffic load only  
 • Observed stresses (principal and second): M. instrum.  
 do. : H  
 do. : M-R

**Erklärungen:** Total berechnete Spannungen (Haupt- und Nebenspannungen)  
 und infolge allein der Verkehrslast (2. Methode)  
 • Gemessene Spannungen (Haupt- und Nebenspannungen): Messapp. M.  
 do. : H  
 do. : M-R

**Montant B-C — Pfosten B-C — Vertikal post B-C**

Echelle des longueurs 1:1.25  
 Echelle des efforts 1 mm = 1.25 kg/mm<sup>2</sup>  
 Längenmaßstab 1:1.25  
 Kräftemaßstab 1 mm = 1.25 kg/mm<sup>2</sup>  
 Scale 1:1.25  
 Scale of stresses 1 mm = 1.25 kg/mm<sup>2</sup>

Effort principal calculé dû à la surcharge seule: + 1.81 kg/mm<sup>2</sup>  
 Berechnete Hauptspannungen infolge allein der Verkehrslast: + 1.81 kg/mm<sup>2</sup>  
 Calculated stresses due to external loadings only: + 1.81 kg/mm<sup>2</sup>

Table XIII.

### Summary.

The experiments have shown that:

1) In the diagonals the measured secondary stresses are of the same order as the calculated secondary stresses, and differ relatively little according to what instruments are used for measuring them. The effect of the gussets is smaller in the case of the diagonals than in that of the verticals. This confirms the fact, which can also be justified on other grounds, that it is better wherever possible to choose the type of bridge made up of sloping elements forming V — shapes in preference to that containing vertical members forming N — shapes.

2) In the verticals the measured secondary stresses vary greatly according to the type of instrument used in their measurement. With some instruments and on certain sections they reach 177 % of the measured principal stress. This may be accounted for:

- a) By the arrangement of the structure, which may have some effect on the distribution of stresses over the area of the section.
- b) By the presence of the large gussets which serve to connect these verticals with the booms.

On turning back to the investigation of the triangulated bridge in reinforced concrete as cited above, it will be seen that the secondary stresses are less in reinforced concrete than in steel. This appears to be attributable to the absence of gussets in reinforced concrete, and to the favourable conditions of transmission of the stresses at the intersection therein.

Leere Seite  
Blank page  
Page vide